STRAY CAPACITANCES OF SINGLE-LAYER AIR-CORE INDUCTORS FOR HIGH-FREQUENCY APPLICATIONS

G. Grandi[1], M.K. Kazimierczuk[2], A. Massarini[3], U. Reggiani[1]

[1]*University of Bologna, Dept. of Electrical Engineering, viale Risorgimento 2, 40136 - Bologna (IT)*
Tel. +39 51 644 3571, fax. +39 51 644 3588, E-mail: elettrot5@ingbo1.ing.unibo.it

[2]*Wright State University, Dept. of Electrical Engineering, Dayton, OH 45435 (USA)*
Tel. +1 513 873 5059, fax. +1 513 873 5009, E-mail: mkazim@valhalla.cs.wright.edu

[3]*University of Modena, Dept. of Engineering Sciences, via Campi 213/B, 41100 - Modena (IT)*
Tel. +39 59 374057, fax. +39 59 364132, E-mail: massarini@eletb2.ing.unibo.it

Abstract - **A method for predicting stray capacitances of HF inductors dependent on their geometry is presented. The analysis is performed for inductors made of one layer of turns with circular and rectangular cross sections. The wire is uniformly wound around a cylindrical non-ferromagnetic core. The method is based on an analytical approach to obtain the turn-to-turn and turn-to-shield capacitances of coils. The influence of insulating coatings of the wire is also taken into account. An overall equivalent stray capacitance is derived according to the typical HF equivalent lumped parameter circuit of inductors. The method was tested with experimental measurements and the accuracy of the results was good in most cases. The derived expressions are useful for designing of HF inductors and can be also used for simulation purposes.**

I. INTRODUCTION

At high frequencies, the behavior of an inductor is very different from its ac low-frequency behavior. In fact, skin and proximity effects cause the winding resistance to increase and the inductance to decrease for increasing operating frequencies. Furthermore, the parasitic capacitances of the windings cannot be neglected at high frequencies.

Parasitic capacitances significantly affect the inductor behavior and are responsible for resonant frequencies. Unfortunately, above its first self-resonant frequency, an inductor behaves like a capacitor. Therefore, in order to obtain an accurate prediction of the response of inductors that operate at frequencies above several hundred kilohertz, such as in EMC filters, RF power amplifiers and radio transmitters, the prediction of stray capacitances is crucial for the design of high-frequency inductors. However, the parasitic capacitances are distributed parameters and predicting the frequency response of an inductor is a difficult task. The high-frequency behavior of wound components is widely discussed in the literature, but mainly the aspects related to the parasitic ac resistance of the winding have been addressed [1]-[3].

Some results concerning stray capacitances of single-layer and multiple-layer coils are presented in [4]-[8]. These works offer some interesting physical insights, but their results relay on some experimental data. A novel simplified method to evaluate the stray capacitances of inductors is presented in [9] and [10]. This method is suited for multiple-layer windings consisting of layers of turns which are close to one another, and a ferromagnetic core. Yet, the method is not sufficiently accurate when the inductor consists of only one layer of turns without a ferromagnetic core and the distance between turns is increased.

The purpose of this paper is to present a method for calculating stray capacitances of single-layer air-core inductors using an analytical approach based on few simplifying assumptions. The presence of a shield is taken into account. The proposed method can predict the overall stray capacitance of an inductor as a function of its geometry only.

II. THE PROPOSED METHOD

A. Basic Assumptions

In EMC filtering applications, the frequencies of interest can range up to tens of megahertz. In order to minimize the effects of parasitic capacitances, inductors are usually made of a single wire wound as a single-layer solenoid and no ferromagnetic core is used. Hence, these inductors have neither turn-to-turn capacitances between turns of different layers, nor turn-to-core capacitances. Furthermore, an air core does not introduce hysteresis and eddy current losses. Wires with both circular and rectangular cross sections are used. The distance between turns is usually increased enough to reduce turn-to-turn capacitances. Inductors for EMC applications, such as those used in Line Impedance Stabilizing Networks (LISN), are usually surrounded by an external shield. The presence of an external shield can give some contribution to the overall stray capacitance of such an inductor.

In this paper, it is assumed that the overall stray capacitance of an inductor can be modeled by a lumped capacitance C connected between the terminals of the winding. The assumed lumped parameter equivalent circuit of an inductor is shown in Fig. 1. The coil inductance and resistance are also depicted in the figure as lumped parameters L and R, respectively.

0-7803-3544-9/96 $5.00

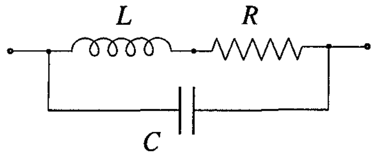

Fig. 1 - Simplified HF model of inductors.

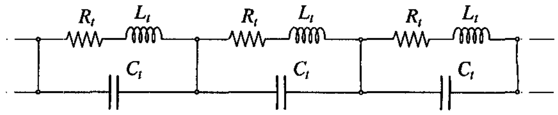

Fig. 3 - Simplified HF distributed equivalent circuit.

The lumped parameter circuit model shown in Fig. 1 can be obtained from a HF equivalent circuit with distributed parameters. The structure of a portion of this circuit is shown in Fig. 2.

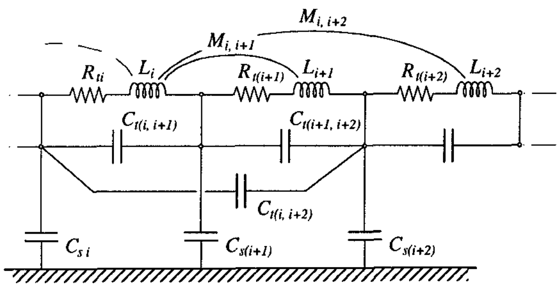

Fig. 2 - HF distributed equivalent circuit for a single-layer air-core inductor with a shield.

The stray capacitances of a single-layer air-core inductor depicted in Fig. 2 are

- turn-to-turn capacitances ($C_{t(i,\ i+1)}$, ...),
- turn-to-shield capacitances (C_{si}, ...).

In Fig. 2, R_{ti} and L_i are the resistance and the inductance of the i-th turn, respectively. $M_{i,i+1}$ and $M_{i,i+2}$ represent the mutual inductances between pairs of turns.

Because of symmetries of the winding, $R_{ti} = R_{t(i+1)} = ... = R_t = R/n$, where n is the number of turns, $C_{t(i,i+1)} = C_{t(i+1,i+2)} = ... = C_t$ and $C_{si} = C_{s(i+1)} = ... = C_s$. In order to obtain the lumped parameter circuit of Fig. 1, the following assumptions are made:

1. For the windings of interest, capacitances between non adjacent turns are small compared to capacitances between adjacent turns. As a consequence, the capacitances between non adjacent turns (of the type of $C_{t(i,i+2)}$ shown in Fig. 2) can be neglected. Moreover, the distance between the coil and the shield is usually large enough so that we can neglect the turn-to-shield capacitances C_{si}.
2. The same current flows through all the turns. This means that edge effects are neglected and each turn has the same series equivalent inductance, L_{ti}, which equals the coil overall inductance L divided by the number of turns ($L_{ti} = L_{t(i+1)} = ...= L_t = L/n$).

Under these assumptions, the equivalent circuit of Fig. 2 can be simplified as shown in Fig. 3. In this circuit, the voltage distribution along the winding is uniform and the parameter values of the model of Fig. 1 satisfy the following relations

$$L = nL_t\ ,\quad R = nR_t\ ,\quad C = C_t/(n\text{-}1). \tag{1}$$

Yet, in the VHF ranges, the impedances of the *RLM* branches of the equivalent circuit of Fig. 2 are much higher of the impedances of the shunt capacitances C_t. As a consequence, the equivalent circuit becomes a capacitor network [11] as shown in Fig. 4. The overall stray capacitance C can be calculated as explained further in Sec. III-C, where also the turn-to-shield capacitances (if they can significantly affect the overall stray capacitance) can be easily taken into account.

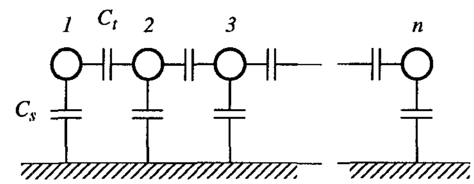

Fig. 4 - VHF equivalent circuit for a single-layer air-core inductor with a shield.

In the next section, an analytical method for calculating the turn-to-turn capacitance C_t and the turn-to-shield capacitance C_s is presented.

B. Calculation of Distributed Capacitances

The cross-sectional view of uniformly wound wires, of either circular or rectangular cross sections, and shields is shown in Fig. 5.

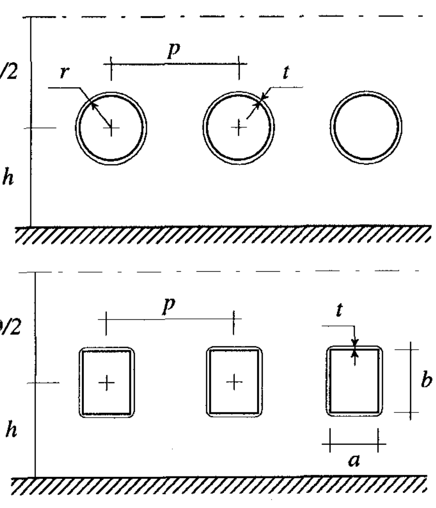

Fig. 5 - Cross-sectional view of coils and shields.

In order to carry out the analysis of such inductors, we assume that turn-to-turn capacitances can be calculated by the capacitance per unit length of two infinitely long straight parallel conductors placed in a homogeneous medium, thus neglecting the turn curvature. Under the previous assumption and if the thickness t of the insulating coating is small compared with the air-gap (p-$2r$), an analytical expression for the turn-to-turn capacitance C_t can be derived for wires of circular cross section [12] as

$$C_t = \frac{\pi^2 D \varepsilon_o}{ln\left(p/2r + \sqrt{(p/2r)^2 - 1}\right)}, \tag{2}$$

where D is the turn diameter, p is the winding pitch (i.e., the distance between the centerlines of two adjacent turns) and r is the wire radius.

When the thickness t of an insulating coating of relative permittivity ε_r is significant, the following expression can be obtained assuming a radial field in the insulating coating

$$C_t = \frac{\pi^2 D \varepsilon_o}{ln\left(F + \sqrt{F^2 - (1 + t/r)^{2/\varepsilon_r}}\right)}, \tag{3}$$

where

$$F = \frac{p/2r}{(1 - t/r)^{1 - 1/\varepsilon_r}}. \tag{4}$$

A detailed derivation of (3) is given in the Appendix.

Similarly, for wires of rectangular cross section it is possible to obtain the following expression assuming the parallel-plate capacitor formula

$$C_t = k\,\varepsilon_o \frac{\pi D b}{p - a}, \tag{5}$$

where k is a factor accounting for edge effects which is a function of the winding geometry. Equation (5) is obtained neglecting the contribution of the insulating coating thickness. If the thickness of the insulating coating is significant, it is possible to modify (5) obtaining the following result

$$C_t = k\,\varepsilon_o \frac{\pi D b}{p - a - 2t\left(1 - 1/\varepsilon_r\right)}. \tag{6}$$

We can evaluate the turn-to-shield capacitances of the structure by neglecting the curvature of both the turns and shield. Under this assumption and neglecting the contribution from the insulating coating, we can calculate the turn-to-shield capacitance C_s through the capacitance per unit length between an infinitely long straight conductor and a parallel conducting plane given by [12]

$$C_s = \frac{2\pi^2 D \varepsilon_o}{ln\left(h/r + \sqrt{(h/r)^2 - 1}\right)}. \tag{7}$$

C. Calculation of the Overall Stray Capacitance

For the equivalent circuit shown in Fig. 3, the overall stray capacitance C is given by (1). In order to evaluate the overall stray capacitance C of the equivalent circuit depicted in Fig. 4, the conducting shield can be regarded as a single node where all the turn-to-shield capacitances C_s are connected and the symmetries of the circuit can be exploited. In fact, for a coil with an even number of turns, we firstly can consider the two turns in the middle of the winding. For these two turns, the capacitor network consists of the capacitance between the two turns, in parallel with the series combination of the turn-to-shield capacitances. The equivalent capacitance of this network is

$$C(2) = C_t + C_s/2. \tag{8}$$

For coils consisting of an odd number of turns, we first consider the three turns placed in the middle of the winding. The equivalent capacitance of the network associated with these three turns is given by

$$C(3) = C_t/2 + C_s/2. \tag{9}$$

In order to get the overall capacitance for coils consisting of any number of turns, we observe that adding one more turn at each side of the above-mentioned turns, the overall capacitance of the previous arrangement is in series with two more turn-to-turn capacitances and then in parallel with the series combination of two more turn-to-shield capacitances. Thus, for n turns we have

$$C(n) = \frac{C(n-2)\,C_t/2}{C(n-2) + C_t/2} + C_s/2. \tag{10}$$

Normalizing with respect to C_t and introducing the capacitance ratio $\alpha = C_s/C_t$, (10) becomes

$$\frac{C(n)}{C_t} = \frac{1}{2 + C_t/C(n-2)} + \alpha/2. \tag{11}$$

Starting from (8) and (9), and using (10) or (11), we can calculate the overall capacitances of coils made of either an even or an odd number of turns, respectively. Furthermore, for large values of n, (11) converges to a finite limit as shown in Fig. 7. It can be seen that the convergence is faster for higher values of the ratio α.

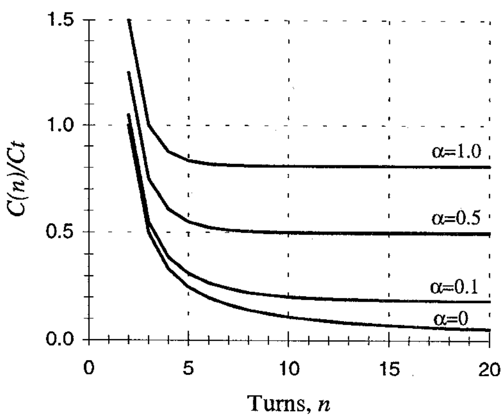

Fig. 7 - Normalized overall capacitance for various values of the ratio α.

It can be found that the convergence limit is related to α through the following expression

$$\frac{C(\infty)}{C_t} = \frac{1}{4}\left(\alpha + \sqrt{\alpha^2 + 4\alpha}\right). \tag{12}$$

Equation (12) is plotted in Fig. 8.

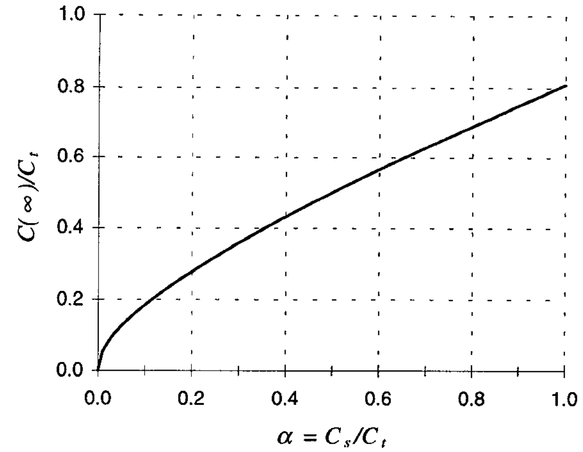

Fig. 8 - Normalized overall capacitance for an infinite number of turns as a function of the capacitance ratio α.

III. Comparison of Numerical and Experimental Results

In order to test the proposed method, single-wire loops without insulating coating were built. These loops of circular cross section were arranged as the turns of a HF coil. This arrangement for n=7 is shown in Fig. 9.

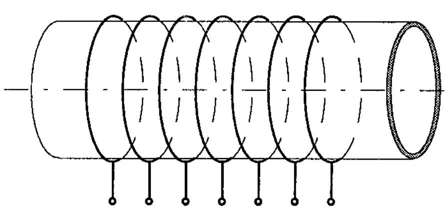

Fig. 9 - Wire loop arrangement for stray capacitance measurements.

Three sets of loops were used for the measurements. The geometrical parameters of the loops are given in Table I. For each set, different pitches were considered. Measured and calculated values for the turn-to-turn capacitance C_t are also given in Table I.

TABLE I
GEOMETRICAL PARAMETERS OF LOOPS

Coil No.	Loop Diameter D [mm]	Wire Radius r [mm]	Pitch p [mm]	Meas. C_t [pF]	Calc. C_t [pF]
1a	47.2	3.25	6.90	11.7	11.82
1b	47.2	3.25	7.32	8.2	8.30
1c	47.2	3.25	9.00	4.7	4.85
2a	36.0	2.70	5.70	9.4	9.48
2b	36.0	2.70	5.98	6.8	6.85
2c	36.0	2.70	7.33	3.8	3.83
3a	26.9	2.12	4.59	5.8	5.82
3b	26.9	2.12	5.05	3.8	3.86
3c	26.9	2.12	6.57	2.3	2.34

The measurements were carried out by means of a HP 4192A LF Impedance Analyzer. As aspected, no significant difference was found for measured capacitances in the range of frequency between 10 kHz and 1 MHz.

The good agreement between the measured and calculated values of the turn-to-turn capacitance C_t indicates that the analytical formula (2) used for the capacitance C_t is accurate. This is valid though in the experimental tests the wire radius was not small compared with the loop diameter.

Fig. 10 shows the measured capacitances for coils of type 1 having four different winding pitches as a function of the turn number.

As turn-to-turn capacitances between non adjacent turns have been neglected in the equivalent circuit of Fig. 3, the measured overall capacitances are larger than the theoretical ones given by (1). For a coil with n=10, the relative error increases from 12% to 23% when the winding pitch increases from 6.90 mm to 16.7 mm.

Figs. 11, 12, and 13 show the measured and theoretical capacitances for the coils a and c of the type 1, 2, and 3, respectively.

The experimental results prove that the proposed HF equivalent circuit of Fig. 3 obtained neglecting the stray capacitances between non adjacent turns, is sufficiently accurate and its accuracy decreases for increasing values of the winding pitch.

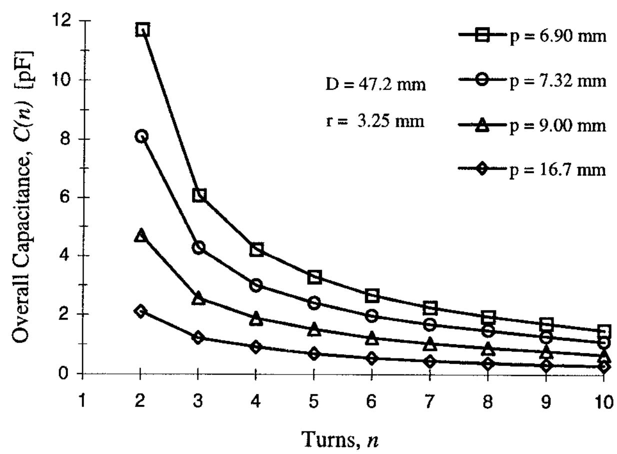

Fig. 10 - Measured capacitances for different values of the winding pitch.

IV. Conclusions

The overall stray capacitance of single-layer air-core inductors was obtained from two simplified equivalent circuits with distributed parameters. The former includes the resistance and the series equivalent inductance of each turn and the turn-to-turn capacitances between adjacent turns. It is valid in HF ranges. The latter consisting of only turn-to-turn and turn-to-shield capacitances, is valid in VHF ranges.

The proposed method for predicting stray capacitances proved to be reliable and suitable for the design and analysis of inductors for high-frequency applications.

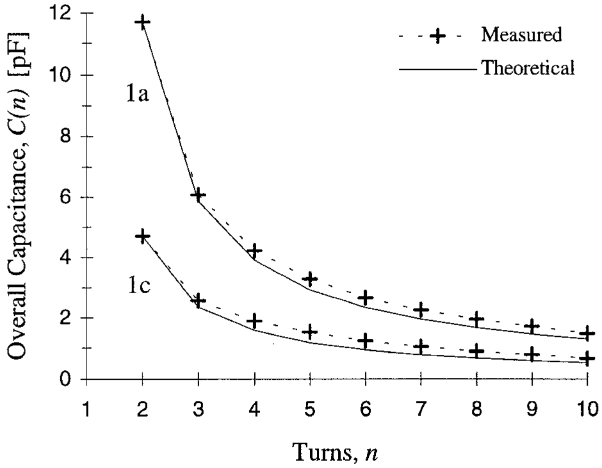

Fig. 11 - Measured and theoretical capacitances as a function of the turn number for the coils 1a and 1c.

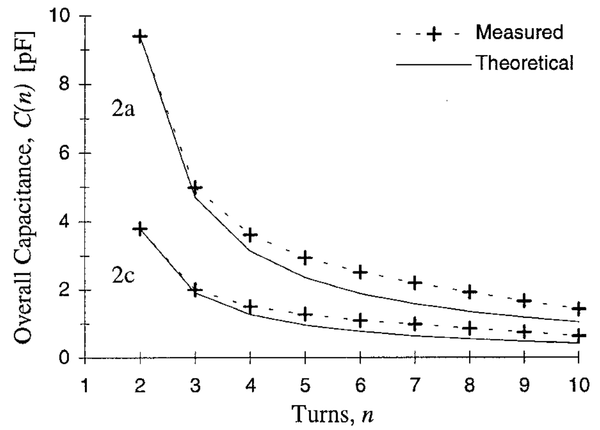

Fig. 12 - Measured and theoretical capacitances as a function of the turn number for the coils 2a and 2c.

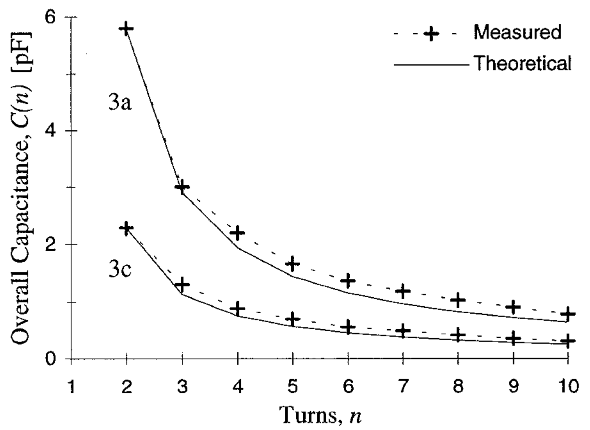

Fig. 13 - Measured and theoretical capacitances as a function of the turn number for the coils 3a and 3c.

REFERENCES

[1] P.L.Dowell, "Effects of eddy currents in transformer windings", *Proc. IEE*, Vol. 113, No. 8, pp. 1287-1394, August 1966.

[2] W.M.Flanagan, *Handbook of Transformer Applications*, McGraw Hill: New York, 1986.

[3] N.R.Grossner, *Transformers for Electronic Circuits*, Second Edition, Mc Graw Hill: New York, 1983

[4] W.T.Duerdoth, "Equivalent capacitances of transformer windings", *Wireless Engr.*, 23, p. 161, 1946.

[5] D.Maurice, and R.H.Minns, "Very-wide-band radio frequency transformers", *Wireless Engr.*, 24, p. 168 (Part I), and p. 209 (Part II), 1947.

[6] K.A.Macfadian, *Small Transformers and Inductors*, Chapman and Hall, Ltd., 1953.

[7] H.Zuhrt, "Einfache Näherungsformeln für die Eigenkapazität Mehrlagiger-Spulen", *Elektrotech. Z.*, 55, p. 662, 1934.

[8] R.G.Medhurst, "H. F. resistance and self-capacitance of single-layer solenoids", *Wireless Engr.*, 24, p. 35, 1947.

[9] A.Massarini, M.K.Kazimierczuk, "Modeling the parasitic capacitance of inductors", CARTS'96, New Orleans, March 1996.

[10] A. Massarini, M.K. Kazimierczuk, and G. Grandi, "Lumped parameter models for single- and multiple-layer inductors", *Proc. Power Electron. Specialist Conf.*, Baveno, June 1996.

[11] M. Kostenko, and L. Piotrovsky, *Electrical Machines*, Vol. 1, Mir, Moscow, 1968.

[12] A.A Zaky, and R. Hawley, *Fundamentals of Electromagnetic Field Theory*, Harrap e Co Ltd.:London, 1974.

APPENDIX

In order to derive (3) of Sec. II-B, we consider the equivalent capacitance of the series combination of the capacitances related to the insulating coatings and the capacitance related to the air-gap between turns. Using the cylindrical capacitor formula, we obtain the per unit length capacitance C_c related to an insulating coating

$$C_c = \frac{2\pi\varepsilon}{ln\,(1+t/r)}. \tag{A1}$$

The per unit length capacitance C_g related to the air-gap can be calculated by means of (2) replacing the wire radius r with the external coating radius $(r + t)$

$$C_g = \frac{\pi\varepsilon_o}{ln\left(\frac{p/2r}{(1+t/r)} + \sqrt{\left(\frac{p/2r}{(1+t/r)}\right)^2 - 1}\right)}. \tag{A2}$$

Using (A1) and (A2), one obtains for the equivalent capacitance per unit length

$$C_{eq} = \frac{C_c C_g}{C_c + 2C_g} = \frac{\pi\varepsilon \cdot \varepsilon_o}{ln\left[(1+t/r)^{\varepsilon_o} \cdot \left(B + \sqrt{B^2 - 1}\right)^{\varepsilon}\right]}, \tag{A3}$$

where $B = \frac{p/2r}{(1+t/r)}$.

We can write the denominator of (A3) in the form

$$ln\left[(1+t/r)^{\varepsilon_o} \cdot \left(B + \sqrt{B^2-1}\right)^{\varepsilon}\right] = \varepsilon \cdot ln\left[(1+t/r)^{\varepsilon_o/\varepsilon} \cdot \left(B + \sqrt{B^2 - 1}\right)\right]. \tag{A4}$$

After few algebraic manipulations and introducing the turn length πD, one obtains (3) of Sec. III-B from (A3) and (A4).